

# Influence of material composition on buckling response of FG plates using a simple plate integral model

Karima Bakhti<sup>1,2</sup>, Mohamed Sekkal<sup>1</sup>, E.A. Adda Bedia<sup>3</sup> and Abdelouahed Tounsi<sup>\*1,3</sup>

<sup>1</sup> Material and Hydrology Laboratory, Faculty of Technology, Civil Engineering Department, University of Sidi Bel Abbès, Algeria

<sup>2</sup> Département de génie civil, Ecole Nationale Polytechnique d'Oran, Algérie

<sup>3</sup> Department of Civil and Environmental Engineering, King Fahd University of Petroleum & Minerals, 31261 Dhahran, Eastern Province, Saudi Arabia

(Received May 22, 2019, Revised September 30, 2019, Accepted November 26, 2019)

**Abstract.** In this study, a simple two-dimensional shear deformation model is employed for buckling analysis of functionally graded (FG) plates. The proposed theory has a kinematic with integral terms which considers the influence of shear deformation without using “shear correction factors”. The impact of varying material properties and volume fraction of the constituent on buckling response of the FG plate is examined and discussed. The benefit of this theory over other contributions is that a number of variables is reduced. The basic equations that consider the influence of transverse shear stresses are derived from the principle of virtual displacements. The analytical solutions are obtained utilizing the “Navier method”. The accuracy of the proposed theory is proved by comparisons with the different solutions found in the literature.

**Keywords:** functionally graded plate; shear deformation theory; buckling

## 1. Introduction

Normally, FGM was created in the 19th century by Japanese research laboratories. They are widely employed in energy sources, aerospace, automotive, nuclear reactor, mechanical, civil, electronic and shipbuilding industries (Kar and Panda 2015a, b, c, d, Kar *et al.* 2016, 2017, Hamed *et al.* 2016, Kar and Panda 2017, Eltaher *et al.* 2018a, Soliman *et al.* 2018). The FGMs are renowned by the continuum and gradual distribution of his material particles through the thickness

In recent decade, different types of FGP structures employed in engineering construction have prompted researchers to develop several plate theories to accurately predict the mechanical behaviours of FG plates (Jha *et al.* 2013). The so-called simplest conventional plate theory (CPT) neglects the transverse shear deformation effect (Mahdavian 2009, Bilouei *et al.* 2016, Eltaher *et al.* 2018b, Avcar and Mohammed 2018) only gives suitable results for thin (flexible) FG-plates and overestimate the results for other thick FG- plates, the 1st shear deformation theory (FSDT) solve the limitation of the CPT and considers the shear deformation effect. For this advantage, several FSDT theories are proposed (Sina *et al.* 2009, Eltaher *et al.* 2014, Mantari and Granados 2015, Hadji *et al.* 2016, Zhao *et al.* 2009a, b, Simsek 2010, Hosseini-Hashemi *et al.* 2011, Pradhan and Chakraverty 2014, Nguyen *et al.* 2017, Chen

and Chang 2018).

In such a formulation, the displacements in the plane vary according to the linear function through the total thickness with constant transverse shear stresses. Therefore, it is necessary to introduce the “*shear correction factor*” to eliminate the unrealistic distribution of transverse shear at free surface of the plate. To avoid the use of shear correction factors, others plate theories are proposed such as higher-order shear deformation model (HSDTs) with nonlinear distribution of displacements (Pradyumna and Bandyopadhyay 2008, Matsunaga 2008, Talha and Singh 2010, Shahrjerdi *et al.* 2011, Reddy 2011, Neves *et al.* 2012a, b, Viswanathan *et al.* 2013, Mantari and Soares 2013, Mehar and Panda 2018, Selmi and Bisharat 2018, Belkacem *et al.* 2018, Batou *et al.* 2019, Safa *et al.* 2019, Sahouane *et al.* 2019, Salah *et al.* 2019, Hadji *et al.* 2019), they can more accurately predict the behaviour of moderate and thick FG plates. Recently, the phenomenon of buckling and postbuckling of structures is more investigated by several authors with considering different types of materials (Emam and Eltaher 2016, Emam *et al.* 2018, Eltaher *et al.* 2019a, b, Mohamed *et al.* 2019).

This work aims to examine the influence of material composition on buckling behaviour of FG plates by employing a simple plate integral model based on HSDT. Adding the integral term to the kinematic reduces the number of variables and governance equations. The material characteristics are continuously varied across the plate thickness according to various power-law functions. The principle of virtual displacements is employed to determine the governing equations and Navier solutions for

\*Corresponding author, Ph.D., Professor,  
E-mail: [tou\\_abdel@yahoo.com](mailto:tou_abdel@yahoo.com)

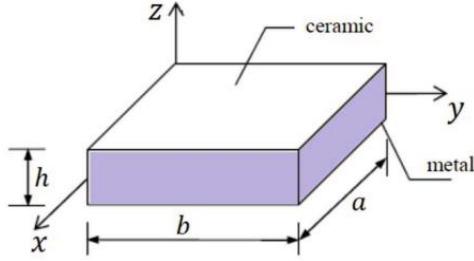


Fig. 1 Typical FGM rectangular plate

FG plates are compared with other existing solutions to check the validity of the present formulation.

## 2. Fundamental formulations

### 2.1 Material gradation

Consider a rectangular FG plate ( $a \times b$ ) of uniform thickness  $h$  (see Fig. 1). The proposed FG plate is made from a mixture of metal and ceramic. The composition of the material varies smoothly in the thickness direction only.

Thus, the modulus of elasticity  $E$  can be expressed by

$$E(z) = E_c V_c + E_m V_m, z \in \left[-\frac{h}{2}, \frac{h}{2}\right] \quad (1)$$

Where  $E_c$  and  $E_m$  are Young's moduli of ceramic and metal,  $V_c$  and  $V_m$  are their volume fractions given by

$$V_c + V_m = 1 \quad (2)$$

The above equations provide an efficient and dimensionless Young's modulus in an appropriate form

$$\bar{E}(z) = \left(\frac{E_c}{E_m} - 1\right) V_c(z) + 1 \quad (3)$$

Where  $\bar{E}(z) = E(z)/E_m$ . Here we suppose that  $V_c$  is according the following different simple power laws (Pitakthapanaphong and Busso 2002, Sofiyev *et al.* 2006, Bouazza *et al.* 2018)

$$V_c = \begin{cases} \frac{z}{h} + \frac{1}{2}, & \text{linear,} \\ \left(\frac{z}{h} + \frac{1}{2}\right)^2, & \text{quadratic,} \\ 3\left(\frac{z}{h} + \frac{1}{2}\right)^2 - 2\left(\frac{z}{h} + \frac{1}{2}\right)^3, & \text{cubic,} \\ 1 - \left(\frac{z}{h} + \frac{1}{2}\right)^2, & \text{inverse quadratic.} \end{cases} \quad (4)$$

### 2.2 Kinematics

On the basis of the thick plate integral model, the following displacement field of the plate can be used as

$$u(x, y, z, t) = u_0(x, y, t) - z \frac{\partial w_0}{\partial x} + k_1 f(z) \int \theta(x, y, t) dx \quad (5a)$$

$$v(x, y, z) = v_0(x, y, t) - z \frac{\partial w_0}{\partial y} + k_2 f(z) \int \theta(x, y, t) dy \quad (5b)$$

$$w(x, y, z, t) = w_0(x, y, t) \quad (5c)$$

where  $u_0, v_0, w_0$  and  $\theta$  are the 4-unknown displacement functions of median surface of the structure. Note that the integrals do not have limits. The constants  $k_1$  and  $k_2$  depends on the geometry. In this study, the shear

$$f(z) = z - \left[ \frac{2z \sinh\left(\frac{z^2}{h^2}\right)}{2 \sinh(1/4) + \cosh(1/4)} \right] \quad (6)$$

$$\text{and } g(z) = \frac{df}{dz}$$

On the basis of the assumptions in Eq. (5), and within the application of the linear theory of elasticity for small deformations, the general deformation-displacement relationships are expressed in

$$\begin{cases} \varepsilon_x \\ \varepsilon_y \\ \gamma_{xy} \end{cases} = \begin{cases} \varepsilon_x^0 \\ \varepsilon_y^0 \\ \gamma_{xy}^0 \end{cases} + z \begin{cases} k_x^b \\ k_y^b \\ k_{xy}^b \end{cases} + f(z) \begin{cases} k_x^s \\ k_y^s \\ k_{xy}^s \end{cases}, \quad (7)$$

$$\begin{cases} \gamma_{yz} \\ \gamma_{xz} \end{cases} = g(z) \begin{cases} \gamma_{yz}^0 \\ \gamma_{xz}^0 \end{cases}$$

where

$$\begin{cases} \varepsilon_x^0 \\ \varepsilon_y^0 \\ \gamma_{xy}^0 \end{cases} = \begin{cases} \frac{\partial u_0}{\partial x} \\ \frac{\partial v_0}{\partial x} \\ \frac{\partial u_0}{\partial y} + \frac{\partial v_0}{\partial x} \end{cases}, \quad \begin{cases} k_x^b \\ k_y^b \\ k_{xy}^b \end{cases} = \begin{cases} -\frac{\partial^2 w_0}{\partial x^2} \\ -\frac{\partial^2 w_0}{\partial y^2} \\ -2\frac{\partial^2 w_0}{\partial x \partial y} \end{cases}, \quad (8a)$$

$$\begin{cases} k_x^s \\ k_y^s \\ k_{xy}^s \end{cases} = \begin{cases} k_1 \theta \\ k_2 \theta \\ k_1 \frac{\partial}{\partial y} \int \theta dx + k_2 \frac{\partial}{\partial x} \int \theta dy \end{cases}$$

$$\begin{cases} \gamma_{yz}^0 \\ \gamma_{xz}^0 \end{cases} = \begin{cases} k_2 \int \theta dy + \frac{\partial \phi_z}{\partial y} \\ k_1 \int \theta dx + \frac{\partial \phi_z}{\partial x} \end{cases} \quad (8b)$$

and

$$g'(z) = \frac{dg(z)}{dz} \quad (8c)$$

It can be observed from Eq. (7) that the transverse shear strains ( $\gamma_{xz}, \gamma_{yz}$ ) become zero at the upper ( $z = h/2$ ) and

lower ( $z = -h/2$ ) faces of the structure. A shear correction coefficient is, thus, not needed the integrals employed in the above equations shall be resolved by a Navier type method and can be expressed as

$$\begin{aligned} \frac{\partial}{\partial y} \int \theta dx &= A \frac{\partial^2 \theta}{\partial x \partial y}, & \frac{\partial}{\partial x} \int \theta dy &= B \frac{\partial^2 \theta}{\partial x \partial y}, \\ \int \theta dx &= A' \frac{\partial \theta}{\partial x}, & \int \theta dy &= B' \frac{\partial \theta}{\partial y} \end{aligned} \quad (9)$$

where coefficients  $A'$  and  $B'$  are considered according to the type of solution employed, in this case via Navier method. Therefore,  $A'$ ,  $B'$ ,  $k_1$  and  $k_2$  are given

$$A' = -\frac{1}{\alpha^2}, \quad B' = -\frac{1}{\beta^2}, \quad k_1 = \alpha^2, \quad k_2 = \beta^2 \quad (10)$$

where  $\alpha$  and  $\beta$  are defined in expression (23).

The linear behavioral relationships of an FG plate as a function of 3D elasticity can be written as follows

$$\begin{Bmatrix} \sigma_x \\ \sigma_y \\ \tau_{xy} \\ \tau_{yz} \\ \tau_{xz} \end{Bmatrix} = \begin{bmatrix} C_{11} & C_{12} & 0 & 0 & 0 \\ C_{12} & C_{22} & 0 & 0 & 0 \\ 0 & 0 & C_{66} & 0 & 0 \\ 0 & 0 & 0 & C_{44} & 0 \\ 0 & 0 & 0 & 0 & C_{55} \end{bmatrix} \begin{Bmatrix} \varepsilon_x \\ \varepsilon_y \\ \gamma_{xy} \\ \gamma_{yz} \\ \gamma_{xz} \end{Bmatrix} \quad (11)$$

The elastic constants ( $C_{ij}$ ) are

$$C_{11} = C_{22} = \frac{E(z)}{(1 - \nu^2)}, \quad (12a)$$

$$C_{12} = \frac{\nu E(z)}{(1 - \nu^2)}, \quad (12b)$$

$$C_{44} = C_{55} = \frac{E(z)}{2(1 + \nu)}, \quad (12c)$$

### 2.3 Equations of equilibrium and stress components

The principle of virtual displacements is considered here to determine the appropriate motion equations and the constitutive equations. The principle can be stated in analytical form in the form

$$0 = \int_0^t (\delta U + \delta V_p) dt \quad (13)$$

where  $\delta U$  is the variation of strain energy;  $\delta V_p$  is the potential energy of applied distributed transverse load. The variation of strain energy of plate is given by

$$\begin{aligned} \delta U &= \int_V [\sigma_x \delta \varepsilon_x + \sigma_y \delta \varepsilon_y + \tau_{xy} \delta \gamma_{xy} \\ &\quad + \tau_{yz} \delta \gamma_{yz} + \tau_{xz} \delta \gamma_{xz}] dV \\ &= \int_A [N_x \delta \varepsilon_x^0 + N_y \delta \varepsilon_y^0 + N_{xy} \delta \gamma_{xy}^0 + M_x^b \delta k_x^0 \end{aligned} \quad (14)$$

$$\begin{aligned} &+ M_y^b \delta k_y^0 + M_{xy}^b \delta k_{xy}^0 + M_{xy}^s \delta L_{xy}^0 \\ &+ S_{yz}^s \delta \gamma_{yz}^0 + S_{xz}^s \delta \gamma_{xz}^0] dA = 0 \end{aligned} \quad (14)$$

where  $A$  is the top surface and the stress resultants  $N$ ,  $M$ ,  $S$ , and  $R$  are defined by

$$\begin{aligned} (N_i, M_i^b, M_i^s) &= \sum_{n=1}^3 \int_{h_n}^{h_{n+1}} (1, z, f) \sigma_i dz, \\ (i = x, y, xy) \quad \text{and} \\ (S_{xz}^s, S_{yz}^s) &= \sum_{n=1}^3 \int_{h_n}^{h_{n+1}} g(\tau_{xz}, \tau_{yz}) dz \end{aligned} \quad (15)$$

Where  $h_{n+1}$  and  $h_n$  are the top and bottom  $z$ -coordinates of the  $n$ th layer.

The variation of the external work can be expressed as

$$\delta V = - \int_A \bar{N} \delta w_0 dA \quad (16a)$$

With

$$\bar{N} = \left[ N_x^0 \frac{\partial^2 w_0}{\partial x^2} + 2N_{xy}^0 \frac{\partial^2 w_0}{\partial x \partial y} + N_y^0 \frac{\partial^2 w_0}{\partial y^2} \right] \quad (16b)$$

where ( $N_x^0, N_y^0, N_{xy}^0$ ) are in-plane applied loads.

By substituting Eqs. (14), (16) into Eq. (13), the following can be derived

$$\begin{aligned} \delta u_0: \quad &\frac{\partial N_x}{\partial x} + \frac{\partial N_{xy}}{\partial y} = 0 \\ \delta v_0: \quad &\frac{\partial N_y}{\partial y} + \frac{\partial N_{xy}}{\partial x} = 0 \\ \delta w_0: \quad &\frac{\partial^2 M_x^b}{\partial x^2} + \frac{\partial^2 M_y^b}{\partial y^2} + 2 \frac{\partial^2 M_{xy}^b}{\partial x \partial y} + \bar{N} = 0 \\ \delta \theta: \quad &-k_1 M_x^s - k_2 M_y^s - (k_1 A' + k_2 B') \frac{\partial^2 M_{xy}^s}{\partial x \partial y} \\ &+ k_1 A \frac{\partial S_{xz}^s}{\partial x} + k_2 B \frac{\partial S_{yz}^s}{\partial y} + \bar{N} = 0 \end{aligned} \quad (17)$$

The stress and moment resultants which appeared in Eq. (15) are given by

$$\begin{Bmatrix} N_x \\ N_y \\ N_{xy} \\ M_x^b \\ M_y^b \\ M_{xy}^b \\ M_x^s \\ M_y^s \\ M_{xy}^s \end{Bmatrix} = \begin{bmatrix} A_{11} & A_{12} & 0 & B_{11} & B_{12} & 0 & B_{11}^s & B_{12}^s & 0 \\ A_{12} & A_{22} & 0 & B_{12} & B_{22} & 0 & B_{12}^s & B_{22}^s & 0 \\ 0 & 0 & A_{66} & 0 & 0 & B_{66} & 0 & 0 & B_{66}^s \\ B_{11} & B_{12} & 0 & D_{11} & D_{12} & 0 & D_{11}^s & D_{12}^s & 0 \\ B_{12} & B_{22} & 0 & D_{12} & D_{22} & 0 & D_{12}^s & D_{22}^s & 0 \\ 0 & 0 & B_{66} & 0 & 0 & D_{66} & 0 & 0 & D_{66}^s \\ B_{11}^s & B_{12}^s & 0 & D_{11}^s & D_{12}^s & 0 & H_{11}^s & H_{12}^s & 0 \\ B_{12}^s & B_{22}^s & 0 & D_{12}^s & D_{22}^s & 0 & H_{12}^s & H_{22}^s & 0 \\ 0 & 0 & B_{66}^s & 0 & 0 & D_{66}^s & 0 & 0 & H_{66}^s \end{bmatrix} \begin{Bmatrix} \frac{\partial u_0}{\partial x} \\ \frac{\partial v_0}{\partial y} \\ \frac{\partial u_0}{\partial y} + \frac{\partial v_0}{\partial x} \\ \frac{\partial^2 w_0}{\partial x^2} \\ \frac{\partial^2 w_0}{\partial y^2} \\ -2 \frac{\partial^2 w_0}{\partial x \partial y} \\ k_1 \theta \\ k_2 \theta \\ (k_1 A' + k_2 B') \frac{\partial^2 \theta}{\partial y^2} \end{Bmatrix} \quad (18a)$$

$$\begin{Bmatrix} S_{yz}^s \\ S_{xz}^s \end{Bmatrix} = \begin{bmatrix} A_{44}^s & 0 \\ 0 & A_{55}^s \end{bmatrix} \begin{Bmatrix} k_2 B' \frac{\partial \theta}{\partial y} \\ k_1 A' \frac{\partial \theta}{\partial x} \end{Bmatrix} \quad (18b)$$

where the stiffness components and are given as

$$(A_{ij}, A_{ij}^s, B_{ij}, D_{ij}, B_{ij}^s, D_{ij}^s, H_{ij}^s) = \int_{-h/2}^{h/2} Q_{ij} \begin{pmatrix} 1, g^2(z), z, z^2, \\ f(z), \\ z f(z), f^2(z) \end{pmatrix} dz \quad (19)$$

Introducing Eqs. (18a), (18b) into Eq. (17), the equations of motion can be expressed in terms of displacements  $(u_0, v_0, w_0, \theta)$  and the appropriate equations take the form

$$\begin{aligned} & A_{11}d_{11}u_0 + A_{66}d_{22}u_0 + (A_{12} + A_{66})d_{12}v_0 \\ & - B_{11}d_{111}w_0 - (B_{12} + 2B_{66})d_{122}w_0 \\ & + (B_{66}^s(k_1A' + k_2B') + B_{12}^s k_2B')d_{122}\theta \\ & + B_{11}^s k_1A'd_{111}\theta = 0, \end{aligned} \quad (20a)$$

$$\begin{aligned} & A_{22}d_{22}v_0 + A_{66}d_{11}v_0 + (A_{12} + A_{66})d_{12}u_0 \\ & - B_{22}d_{222}w_0 - (B_{12} + 2B_{66})d_{112}w_0 \\ & + (B_{66}^s(k_1A' + k_2B') + B_{12}^s k_1A')d_{112}\theta \\ & + B_{22}^s k_2B'd_{222}\theta = 0, \end{aligned} \quad (20b)$$

$$\begin{aligned} & B_{11}d_{111}u_0 + (B_{12} + 2B_{66})d_{122}u_0 \\ & + (B_{12} + 2B_{66})d_{112}v_0 + B_{22}d_{222}v_0 \\ & - D_{11}d_{1111}w_0 - 2(D_{12} + 2D_{66})d_{1122}w_0 \\ & - D_{22}d_{2222}w_0 + D_{11}^s k_1A'd_{1111}\theta \\ & + ((D_{12}^s + 2D_{66}^s)(k_1A' + k_2B'))d_{1122}\theta \\ & + D_{22}^s k_2B'd_{2222}\theta + N_x^0 d_{11}w_0 \\ & + 2N_{xy}^0 d_{12}w_0 + N_y^0 d_{22}w_0 = 0 \end{aligned} \quad (20c)$$

$$\begin{aligned} & -k_1A'^s d_{111}u_0 - (B_{12}^s k_2B' + B_{66}^s(k_1A' + k_2B'))d_{122}u_0 \\ & - (B_{22}^s k_1A' + B_{66}^s(k_1A' + k_2B'))d_{112}v_0 \\ & - B_{22}^s k_2B'd_{222}v_0 + D_{11}^s k_1A'd_{1111}w_0 \\ & + ((D_{12}^s + 2D_{66}^s)(k_1A' + k_2B'))d_{1122}w_0 \\ & + D_{22}^s k_2B'd_{2222}w_0 - H_{11}^s(k_1A')^2 d_{1111}\theta \\ & - H_{22}^s(k_2B')^2 d_{2222}\theta - (2H_{12}^s k_1k_2A'B') \\ & + (k_1A' + k_2B')^2 H_{66}^s d_{1122}\theta \\ & + A_{44}^s(k_1A')^2 d_{11}\theta + A_{55}^s(k_2B')^2 d_{22}\theta = 0 \end{aligned} \quad (20d)$$

where  $d_{ij}$ ,  $d_{ijl}$  and  $d_{ijlm}$  are the following differential operators

$$\begin{aligned} d_{ij} &= \frac{\partial^2}{\partial x_i \partial x_j}, & d_{ijl} &= \frac{\partial^3}{\partial x_i \partial x_j \partial x_l}, \\ d_{ijlm} &= \frac{\partial^4}{\partial x_i \partial x_j \partial x_l \partial x_m}, & d_i &= \frac{\partial}{\partial x_i}, \end{aligned} \quad (21)$$

( $i, j, l, m = 1, 2$ ).

## 2.4 Analytical solution for simply-supported FG plates

The Navier solution procedure is utilized to deduce the analytical solutions for which the displacement variables are given as product of arbitrary parameters and known trigonometric functions to respect the equations of motion and boundary conditions.

$$\begin{Bmatrix} u_0 \\ v_0 \\ w_0 \\ \theta \end{Bmatrix} = \sum_{m=1}^{\infty} \sum_{n=1}^{\infty} \begin{Bmatrix} U_{mn} \cos(\alpha x) \sin(\beta y) \\ V_{mn} \sin(\alpha x) \cos(\beta y) \\ W_{mn} \sin(\alpha x) \sin(\beta y) \\ X_{mn} \sin(\alpha x) \sin(\beta y) \end{Bmatrix} \quad (22)$$

White

$$\alpha = m\pi/a \quad \text{and} \quad \beta = n\pi/b \quad (23)$$

Considering that the plate is subjected to in-plane compressive loads of form:  $N_x^0 = -N_0$ ,  $N_y^0 = -\gamma N_0$ ,  $N_{xy}^0 = 0$ ,  $\gamma = N_y^0/N_x^0$ , (here  $\gamma$  are non-dimensional load parameter).

Substituting Eq. (22) into Eq. (20), the following problem is obtained

$$\begin{pmatrix} S_{11} & S_{12} & S_{13} & S_{14} \\ S_{12} & S_{22} & S_{23} & S_{24} \\ S_{13} & S_{23} & S_{33} + k & S_{34} \\ S_{14} & S_{24} & S_{34} & S_{44} \end{pmatrix} \begin{Bmatrix} U_{mn} \\ V_{mn} \\ W_{mn} \\ X_{mn} \end{Bmatrix} = \begin{Bmatrix} 0 \\ 0 \\ 0 \\ 0 \end{Bmatrix} \quad (24)$$

Where

$$\begin{aligned} S_{11} &= A_{11}\alpha^2 + A_{66}\beta^2, & S_{12} &= \alpha\beta(A_{12} + A_{66}), \\ S_{13} &= -\alpha(B_{11}\alpha^2 + (B_{12} + 2B_{66})\beta^2), \\ S_{14} &= \alpha \left( (k_2B' B_{12}^s + (k_1A' + k_2B')B_{66}^s)\beta^2 \right. \\ &\quad \left. + k_1A' B_{11}^s \alpha^2 \right), \\ S_{22} &= A_{66}\alpha^2 + A_{22}\beta^2, \\ S_{23} &= -\beta(B_{22}\beta^2 + (B_{12} + 2B_{66})\alpha^2), \\ S_{24} &= \beta \left( (k_1A' B_{12}^s + (k_1A' + k_2B')B_{66}^s)\alpha^2 \right. \\ &\quad \left. + k_2B' B_{22}^s \beta^2 \right), \\ S_{33} &= D_{11}\alpha^4 + 2(D_{12} + 2D_{66})\alpha^2\beta^2 + D_{22}\beta^4, \\ S_{34} &= -k_1A'^s D_{11}\alpha^4 - ((D_{12}^s + 2D_{66}^s)(k_1A' + k_2B')) \\ &\quad \alpha^2\beta^2 - k_2B'^s D_{22}\beta^4, \\ S_{44} &= (k_1A')^2 H_{11}^s \alpha^4 + (2k_1k_2A'B'^s H_{12}^s \\ &\quad + (k_1A' + k_2B')^2 H_{66}^s)\alpha^2\beta^2 + (k_2B')^2 H_{22}^s \beta^4 \\ &\quad + (k_2B')^2 A_{55}^s \beta^2 + (k_1A')^2 A_{44}^s \alpha^2, \\ k &= -N_0(\alpha^2 + \gamma\beta^2) \end{aligned} \quad (25)$$

## 3. Numerical results

A simply supported FG rectangular plate is considered here as shown by Fig. 1. FG structures made of two material combinations of metal and ceramic: Al/Al<sub>2</sub>O<sub>3</sub> and Al/SiC are considered. Their material characteristics are presented in Table 1. For convenience, the following non-dimensional parameters are employed

$$\bar{N}_{cr} = \frac{N_{cr}a^2}{E_m h^3}, \quad \hat{N}_{cr} = \frac{N_{cr}a^2}{D_{11} - B_{11}^2/A_{11}} \quad (26)$$

Table 1 Material properties of metal and ceramic

Material	Young's modulus (GPa)	Poisson's ratio
Aluminum (Al)	70	0.3
Alumina (Al <sub>2</sub> O <sub>3</sub> )	380	0.3
Silicon carbide (SiC)	420	0.3

Table 2 Comparison of the critical buckling load ( $\bar{N}_{cr}$ ) of Al/SiC square plates ( $a/h = 10$ )

$\gamma$	Theory	Power law index					
		0	0.5	1	2	5	10
0	Mohammadi <i>et al.</i> (2010)	37.3708	–	37.7132	37.7089	–	–
	Bodaghi and Saidi (2010)	37.3714	–	37.7172	37.5765	–	–
	Nguyen (2015)	37.4215	37.6650	37.7560	37.6327	36.8862	36.5934
	Present	37.3721	37.6301	37.7143	37.6050	36.9227	36.5644
1	Mohammadi <i>et al.</i> (2010)	18.6854	–	18.8566	18.8545	–	–
	Bodaghi and Saidi (2010)	18.6860	–	18.8571	18.8020	–	–
	Nguyen (2015)	18.7107	18.8325	18.8780	18.8163	18.4431	18.2967
	Present	18.6860	18.8150	18.8571	18.8025	18.4613	18.2822
-1	Mohammadi <i>et al.</i> (2010)	72.0834	–	73.6307	73.6112	–	–
	Bodaghi and Saidi (2010)	72.2275	–	73.6645	73.1587	–	–
	Nguyen (2015)	72.3281	73.4526	73.8426	73.2827	69.9876	68.7244
	Present	72.0981	73.2593	73.6435	73.1471	70.1286	68.5990

Three types of in-plane loads are employed: uniaxial compression ( $\gamma = 0$ ), biaxial compressions ( $\gamma = 1$ ) and axial compression and tension ( $\gamma = -1$ ). The computed results are provided in Tables 2 and 3. It is clear that the obtained results agree well with other solutions (FSDT) Mohammadi *et al.* (2010), (HSDT) Bodaghi and Saidi (2010), Sekkal *et al.* (2017) and (HSDT) Nguyen (2015).

Fig. 2 shows the critical buckling loads of square plates with respect to the geometric ratio ( $a/h$ ) for different material distributions ( $V_c$ ). The two cases of isotropic

alumina and aluminum correspond to the fully ceramic plate and fully metallic plate, respectively. However, the other cases of FG plates are defined as follows: linear, quadratic, cubic, and quadratic inverse. In Fig. 2, it is obvious that the variation of critical buckling load ( $\bar{N}_{cr}$ ) of FG plates is greater than that of the fully metal plate (Al) but smaller than that of the fully ceramic plate ( $\text{Al}_2\text{O}_3$ ). It is observed that for uniaxial compression ( $\gamma = 0$ ), biaxial compressions ( $\gamma = 1$ ) and axial compression and tension ( $\gamma = -1$ ), the variation of the critical buckling load obtained from the

Table 3 Comparison of the critical buckling load ( $\bar{N}_{cr}$ ) of Al/ $\text{Al}_2\text{O}_3$  plates

$\gamma$	a/b	a/h	Theory	Power law index				
				0	0.5	1	2	10
0	5		Nguyen (2015)	6.7417	4.4343	3.4257	2.6503	1.9260
			Sekkal <i>et al.</i> (2017)	6.7005	4.4728	3.4983	2.7347	1.9459
			Present	6.7202	4.4234	3.4163	2.6452	1.9215
	10		Nguyen (2015)	7.4115	4.8225	3.7137	2.8911	2.1911
			Sekkal <i>et al.</i> (2017)	7.4126	4.8904	3.8221	3.0168	2.2374
			Present	7.4053	4.8206	3.7110	2.8897	2.1896
	20		Nguyen (2015)	7.6009	4.9307	3.7937	2.9585	2.2695
			Sekkal <i>et al.</i> (2017)	7.6109	5.0028	3.9108	3.0968	2.3230
			Present	7.5992	4.9314	3.7930	2.9581	2.2690
	5		Nguyen (2015)	16.1003	10.6670	8.2597	6.3631	4.4981
			Sekkal <i>et al.</i> (2017)	15.9193	10.7065	8.3828	6.5148	4.5077
			Present	16.0209	10.6252	8.2244	6.3435	4.4815
	10		Nguyen (2015)	18.6030	12.1317	9.3496	7.2687	5.4587
			Sekkal <i>et al.</i> (2017)	18.5846	12.2937	9.6083	7.5667	5.5625
			Present	18.5785	12.1229	9.3391	7.2632	5.4532
	20		Nguyen (2015)	19.3593	12.5652	9.6702	7.5386	5.7689
			Sekkal <i>et al.</i> (2017)	19.3809	12.7494	9.9658	7.8860	5.9020
			Present	19.3527	12.5667	9.6674	7.5371	5.7669

Table 3 Continued

$\gamma$	a/b	a/h	Theory	Power law index					
				0	0.5	1	2	5	10
1	0.5	5	Nguyen (2015)	5.3934	3.5475	2.7406	2.1202	1.7167	1.5408
			Sekkal <i>et al.</i> (2017)	5.3604	3.5783	2.7987	2.1878	1.7661	1.5568
			Present	5.3762	3.5387	2.7330	2.1161	1.7191	1.5372
		10	Nguyen (2015)	5.9292	3.8580	2.9710	2.3129	1.9324	1.7529
			Sekkal <i>et al.</i> (2017)	5.9301	3.9123	3.0577	2.4134	2.0072	1.7899
			Present	5.9242	3.8565	2.9688	2.3117	1.9333	1.7517
		20	Nguyen (2015)	6.0807	3.9445	3.0350	2.3668	1.9953	1.8156
			Sekkal <i>et al.</i> (2017)	6.0887	4.0022	3.1287	2.4774	2.0770	1.8584
			Present	6.0794	3.9451	3.0344	2.3665	1.9955	1.8152
	1	5	Nguyen (2015)	8.0501	5.3335	4.1299	3.1815	2.5230	2.2491
			Sekkal <i>et al.</i> (2017)	7.9597	5.3533	4.1914	3.2574	2.5763	2.2539
			Present	8.0104	5.3126	4.1122	3.1717	2.5273	2.2407
		10	Nguyen (2015)	9.3015	6.0659	4.6748	3.6344	3.0158	2.7293
			Sekkal <i>et al.</i> (2017)	9.2923	6.14687	4.8042	3.7834	3.1268	2.78123
			Present	9.2892	6.0614	4.6695	3.6316	3.0179	2.7266
		20	Nguyen (2015)	9.6796	6.2826	4.8351	3.7693	3.1718	2.8844
			Sekkal <i>et al.</i> (2017)	9.6904	6.3747	4.9829	3.9430	3.3004	2.9510
			Present	9.6763	6.2833	4.8337	3.7685	3.1724	2.8834
-1	0.5	5	Nguyen (2015)	8.9890	5.9124	4.5676	3.5337	2.8612	2.5679
			Sekkal <i>et al.</i> (2017)	8.9339	5.9637	4.6645	3.6463	2.9435	2.5946
			Present	8.9603	5.8979	4.5551	3.5269	2.8652	2.5620
		10	Nguyen (2015)	9.8820	6.4299	4.9516	3.8548	3.2206	2.9214
			Sekkal <i>et al.</i> (2017)	9.8835	6.5206	5.0962	4.0224	3.3453	3.3453
			Present	9.8737	6.4275	4.9481	3.8529	3.2221	2.9195
		20	Nguyen (2015)	10.1345	6.5742	5.0583	3.9447	3.3255	3.0260
			Sekkal <i>et al.</i> (2017)	10.1478	6.6704	5.2145	4.1291	3.4617	3.0974
			Present	10.1323	6.5752	5.0574	3.9442	3.3259	3.0253
	1	5	Nguyen (2015)	26.4999	17.9424	13.9872	10.6421	7.9571	6.9626
			Sekkal <i>et al.</i> (2017)	25.7567	17.6913	13.9068	10.6372	7.9346	6.8033
			Present	26.2039	17.7691	13.8477	10.5596	7.96344	6.8989
		10	Nguyen (2015)	35.9559	23.6497	18.2704	14.1349	11.4447	10.2717
			Sekkal <i>et al.</i> (2017)	35.7357	23.8550	18.6579	14.5850	11.7741	10.3784
			Present	35.8415	23.5918	18.2205	14.1079	11.4610	10.2483
		20	Nguyen (2015)	39.5280	25.7197	19.8065	15.4190	12.8824	11.6857
			Sekkal <i>et al.</i> (2017)	39.5339	26.0822	20.3846	16.0896	13.3813	11.9329
			Present	39.4951	25.7100	19.7925	15.4117	12.8886	11.6783

quadratic compositional profile, is lower than cubic, linear and inverse quadratic cases.

Fig. 3 presents the critical buckling loads of plates with respect to the geometric ratio ( $a/b$ ) for different material distributions ( $V_c$ ). Again, it is obvious that the variation of critical buckling load ( $\bar{N}_{cr}$ ) of FG plates is greater than that of the fully metal plate (Al) but smaller than that of the fully ceramic plate ( $\text{Al}_2\text{O}_3$ ). It is also observed that the variation of the critical buckling load

obtained from the quadratic distribution is lower than cubical, linear and inverse quadratic cases. Therefore, quadratic distribution makes the plate more flexible than other distributions.

A comparison of critical buckling loads of the FG rectangular and square plate is presented in Figs. 4 and 5 for various moduli ratios ( $E_m/E_c$ ). It is observed that with increasing of the modulus ratio  $E_m/E_c$  from 0.05 to 0.5, the critical buckling loads decrease steadily. However, it is

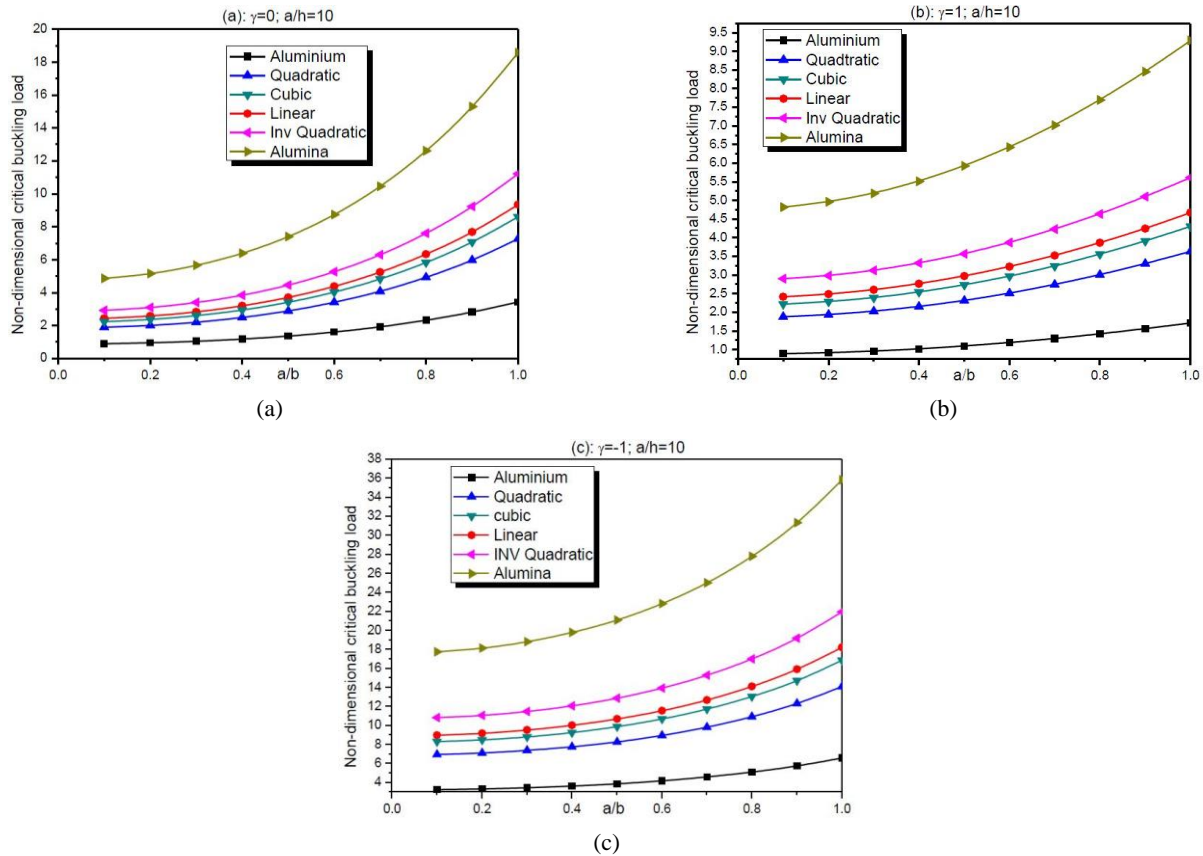


Fig. 2 Non-dimensional critical buckling load ( $\bar{N}_{cr}$ ) for metal, ceramic and FGM plates versus sides to thickness ratio ( $a/h$ ) for different compositional profiles

observed that critical buckling loads of the quadratic case are lower than those of cubic, linear, and inverse quadratic cases.

#### 4. Conclusions

In this work, a higher-order hyperbolic shear deformation integral plate theory is presented and proposed for analysing the effect of material composition on buckling response of FG plates. The gradation of material properties

within thickness is considered to be of various power-law functions type (linear, quadratic, cubic, and inverse quadratic) and comparisons are carried out with homogeneous metal and ceramic plates. It is seen that the basic behaviour of FG plates that correspond to characteristics intermediate to that of metal and ceramic, is necessarily laid in between that of metal and ceramic. In conclusion, it can be observed that gradients in material properties play a considerable role in determining response of FG material plates, and the proposed higher-order hyperbolic shear deformation integral plate theory is simple

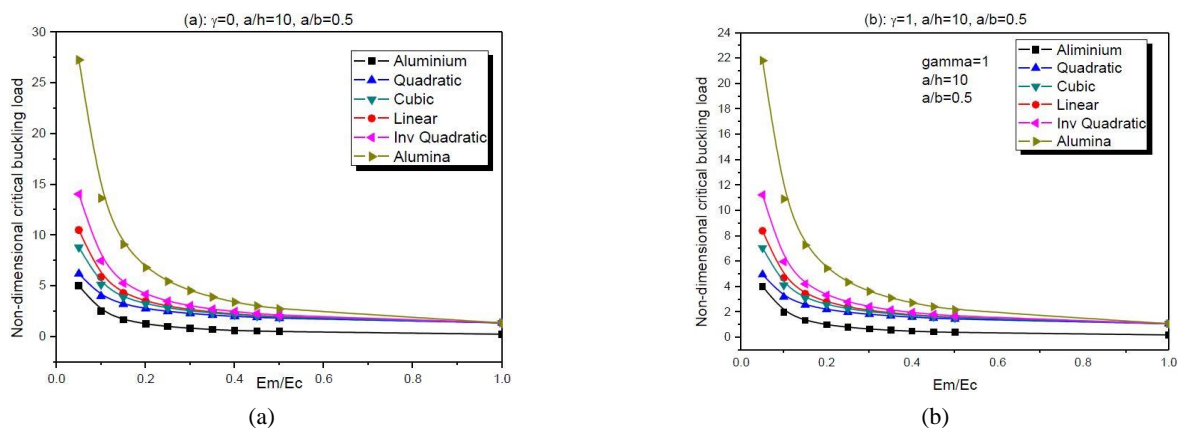


Fig. 3 Non-dimensional critical buckling load ( $\bar{N}_{cr}$ ) for metal, ceramic and FGM plates versus sides to geometric ratio ( $a/b$ ) for different compositional profiles

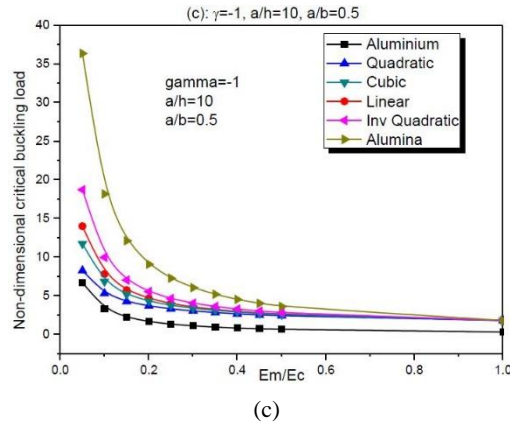
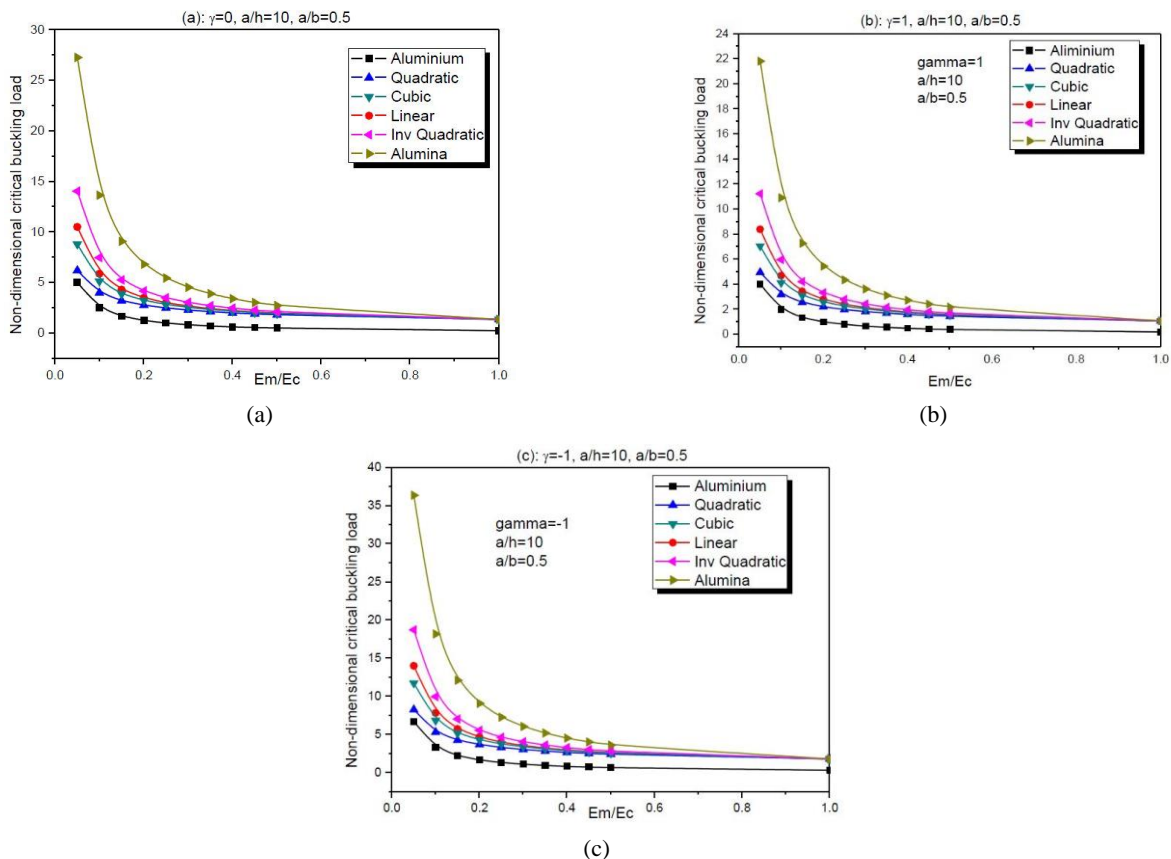


Fig. 3 Continued

Fig. 4 The effect of material anisotropy on the non-dimensional critical buckling load ( $\bar{N}_{cr}$ ) of an FGM rectangular plate for different compositional profiles

and accurate in resolving buckling responses of FGM plates.

## References

- Avcar, M. and Mohammed, W.K.M. (2018), "Free vibration of functionally graded beams resting on Winkler-Pasternak foundation", *Arab. J. Geosci.*, **11**(10), 232.  
<https://doi.org/10.1007/s12517-018-3579-2>
- Batou, B., Nebab, M., Bennai, R., AitAtmane, H., Tounsi, A. and Bouremana, M. (2019), "Wave dispersion properties in imperfect sigmoid plates using various HSDTs", *Steel Compos. Struct.*, **33**(5), 699-716.  
<https://doi.org/10.12989/scs.2019.33.5.699>
- Belkacem, A., Tahar, H.D., Abderrezak, R., Amine, B.M., Mohamed, Z. and Boussad, A. (2018), "Mechanical buckling analysis of hybrid laminated composite plates under different boundary conditions", *Struct. Eng. Mech.*, **66**(6), 761-769.  
<https://doi.org/10.12989/sem.2018.66.6.761>
- Bilouei, B.S., Kolahchi, R. and Bidgoli, M.R. (2016), "Buckling of concrete columns retrofitted with Nano-Fiber Reinforced Polymer (NFRP)", *Comput. Concrete, Int. J.*, **18**(5), 1053-1063.  
<https://doi.org/10.12989/cac.2016.18.5.1053>
- Bodaghi, M. and Saidi, A.R. (2010), "Levy-type solution for buckling analysis of thick functionally graded rectangular plates



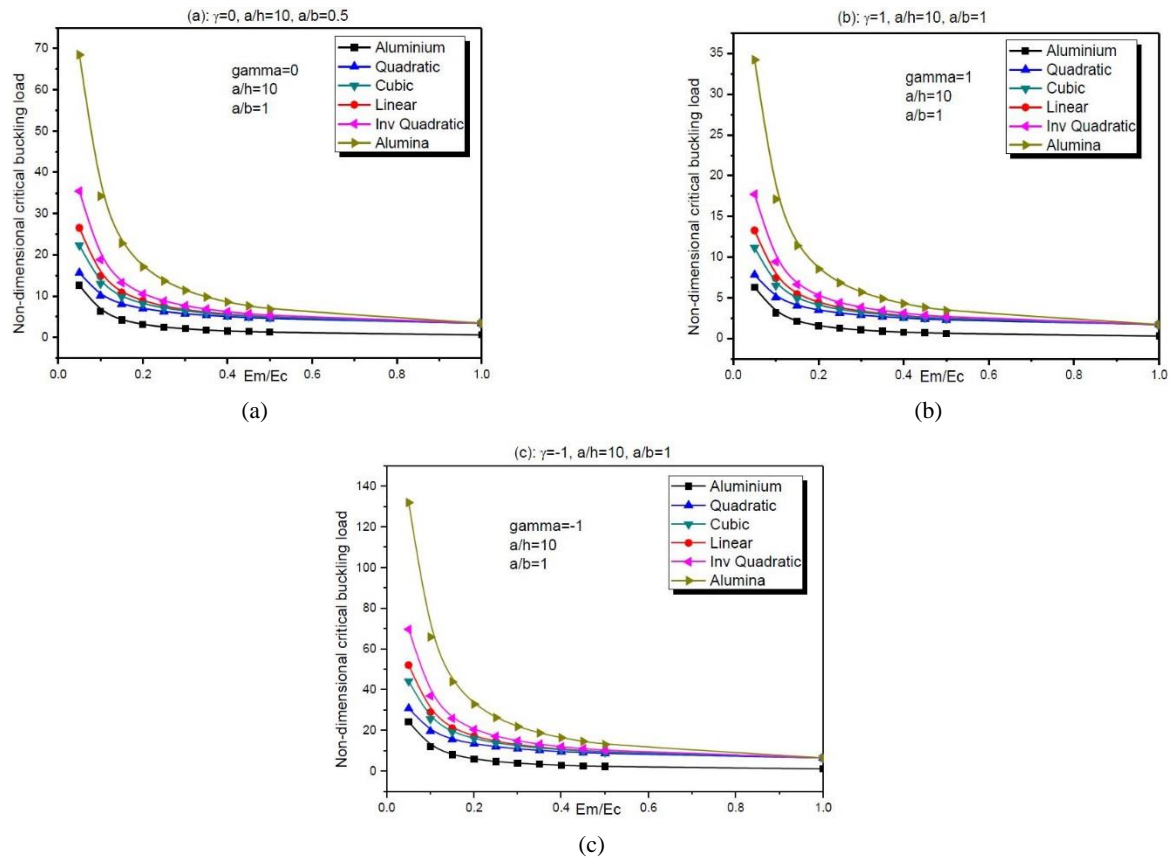


Fig. 5 The effect of material anisotropy on the non-dimensional critical buckling load ( $\bar{N}_{cr}$ ) of an FGM square plate for different compositional profiles

- based on the higher-order shear deformation plate theory”, *Appl. Math. Model.*, **34**, 3659-3673.  
<https://doi.org/10.1016/j.apm.2010.03.016>
- Bouazza, M., Zenkour, A.M. and Benseddiq, N. (2018), “Effect of material composition on bending analysis of FG plates via a two-variable refined hyperbolic theory”, *Arch. Mech.*, **70**(2), 107-129.
- Chen, W.R. and Chang, H. (2018), “Vibration analysis of functionally graded timoshenko beams”, *Int. J. Struct. Stab. Dyn.*, **18**, 1850007. <https://doi.org/10.1142/S0219455418500074>
- Eltaher, M.A., Khairy, A., Sadoun, A.M. and Omar, F.A. (2014), “Static and buckling analysis of functionally graded Timoshenko nanobeams”, *Appl. Mathe. Comput.*, **229**, 283-295.  
<https://doi.org/10.1016/j.amc.2013.12.072>
- Eltaher, M.A., Attia, M.A., Soliman, A.E. and Alshorbagy, A.E. (2018a), “Analysis of crack occurs under unsteady pressure and temperature in a natural gas facility by applying FGM”, *Struct. Eng. Mech., Int. J.*, **66**(1), 97-111.  
<https://doi.org/10.12989/sem.2018.66.1.097>
- Eltaher, M.A., Fouda, N., El-midany, T. and Sadoun, A.M. (2018b), “Modified porosity model in analysis of functionally graded porous nanobeams”, *J. Brazil. Soc. Mech. Sci. Eng.*, **40**(3), 141. <https://doi.org/10.1007/s40430-018-1065-0>
- Eltaher, M.A., Mohamed, N., Mohamed, S.A. and Seddek, L.F. (2019a), “Periodic and nonperiodic modes of postbuckling and nonlinear vibration of beams attached to nonlinear foundations”, *Appl. Mathe. Model.*, **75**, 414-445.  
<https://doi.org/10.1016/j.apm.2019.05.026>
- Eltaher, M.A., Mohamed, N., Mohamed, S. and Seddek, L.F. (2019b), “Postbuckling of curved carbon nanotubes using energy equivalent model”, *J. Nano Res.*, **57**, 136-157.  
<https://doi.org/10.4028/www.scientific.net/JNanoR.57.136>
- Emam, S. and Eltaher, M.A. (2016), “Buckling and postbuckling of composite beams in hygrothermal environments”, *Compos. Struct.*, **152**, 665-675.  
<https://doi.org/10.1016/j.compstruct.2016.05.029>
- Emam, S., Eltaher, M.A., Khater, M. and Abdalla, W. (2018), “Postbuckling and free vibration of multilayer imperfect nanobeams under a pre-stress load”, *Appl. Sci.*, **8**(11), 2238.  
<https://doi.org/10.3390/app8112238>
- Hadji, L., Hassaine Daouadji, T., Ait Amar Meziane, M., Tlidji, Y. and Adda Bedia, E.A. (2016), “Analysis of functionally graded beam using a new first-order shear deformation theory”, *Struct. Eng. Mech., Int. J.*, **57**(2), 315-325.  
<https://doi.org/10.12989/sem.2016.57.2.315>
- Hadji, L., Zouatnia, N. and Bernard, F. (2019), “An analytical solution for bending and free vibration responses of functionally graded beams with porosities: Effect of the micromechanical models”, *Struct. Eng. Mech., Int. J.*, **69**(2), 231-241.  
<https://doi.org/10.12989/sem.2019.69.2.231>
- Hamed, M.A., Eltaher, M.A., Sadoun, A.M. and Almitani, K.H. (2016), “Free vibration of symmetric and sigmoid functionally graded nanobeams”, *Appl. Phys. A*, **122**(9), 829.  
<https://doi.org/10.1007/s00339-016-0324-0>
- Hosseini-Hashemi, S., Fadaee, M. and Atashipour, S.R. (2011), “A new exact analytical approach for free vibration of Reissner-Mindlin functionally graded rectangular plates”, *Int. J. Mech. Sci.*, **53**, 11-22. <https://doi.org/10.1016/j.ijmecsci.2010.10.002>
- Jha, D.K., Kant, T. and Singh, R.K. (2013), “A critical review of recent research on functionally graded plates”, *Compos. Struct.*, **96**, 833-849. <https://doi.org/10.1016/j.compstruct.2012.09.001>
- Kar, V.R. and Panda, S.K. (2015a), “Thermoelastic analysis of functionally graded doubly curved shell panels using nonlinear finite element method”, *Compos. Struct.*, **129**, 202-212.

- <https://doi.org/10.1016/j.compstruct.2015.04.006>
- Kar, V.R. and Panda, S.K. (2015b), "Free vibration responses of temperature dependent functionally graded curved panels under thermal environment", *Latin Am. J. Solids Struct.*, **12**(11), 20062024. <https://doi.org/10.1590/1679-78251691>
- Kar, V.R. and Panda, S.K. (2015c), "Large deformation bending analysis of functionally graded spherical shell using FEM", *Struct. Eng. Mech.*, *Int. J.*, **53**(4), 661-679. <https://doi.org/10.12989/sem.2015.53.4.661>
- Kar, V.R. and Panda, S.K. (2015d), "Nonlinear flexural vibration of shear deformable functionally graded spherical shell panel", *Steel Compos. Struct.*, *Int. J.*, **18**(3), 693-709. <https://doi.org/10.12989/scs.2015.18.3.693>
- Kar, V.R. and Panda, S.K. (2017), "Large-amplitude vibration of functionally graded doubly-curved panels under heat conduction", *AIAA J.*, **55**(12), 4376-4386. <https://doi.org/10.2514/1.J055878>
- Kar, V.R., Panda, S.K. and Mahapatra, T.R. (2016), "Thermal buckling behaviour of shear deformable functionally graded single/doubly curved shell panel with TD and TID properties", *Adv. Mater. Res.*, *Int. J.*, **5**(4), 205-221. <https://doi.org/10.12989/amr.2016.5.4.205>
- Kar, V.R., Mahapatra, T.R. and Panda, S.K. (2017), "Effect of different temperature load on thermal postbuckling behaviour of functionally graded shallow curved shell panels", *Compos. Struct.*, **160**, 1236-1247. <https://doi.org/10.1016/j.compstruct.2016.10.125>
- Mahdavian, M. (2009), "Buckling analysis of simply-supported functionally graded rectangular plates under non-uniform inplane compressive loading", *J. Solid Mech.*, **1**, 213-225.
- Mantari, J.L. and Granados, E.V. (2015), "A refined FSDT for the static analysis of functionally graded sandwich plates", *Thin Wall. Struct.*, **90**, 150-158. <https://doi.org/10.1016/j.tws.2015.01.015>
- Mantari, J. and Soares, C.G. (2013), "A novel higher-order shear deformation theory with stretching effect for functionally graded plates", *Compos. Part B*, **45**(1), 268-281. <https://doi.org/10.1016/j.compositesb.2012.05.036>
- Mantari, J.L., Oktem, A.S. and Soares, O.G. (2012), "Bending response of functionally graded plates by using a new higher order shear deformation theory", *Compos. Struct.*, **94**, 714-723. <https://doi.org/10.1016/j.compstruct.2011.09.007>
- Matsunaga, H. (2008), "Free vibration and stability of functionally graded plates according to a 2D higher-order deformation theory", *Compos. Struct.*, **82**, 499-512. <https://doi.org/10.1016/j.compstruct.2007.01.030>
- Mehar, K. and Panda, S.K. (2018), "Nonlinear finite element solutions of thermoelastic flexural strength and stress values of temperature dependent graded CNT-reinforced sandwich shallow shell structure", *Struct. Eng. Mech.*, *Int. J.*, **67**(6), 565-578. <https://doi.org/10.12989/sem.2018.67.6.565>
- Mohamed, N., Eltaher, M.A., Mohamed, S. and Seddek, L.F. (2019), "Energy equivalent model in analysis of postbuckling of imperfect carbon nanotubes resting on nonlinear elastic foundation", *Struct. Eng. Mech.*, *Int. J.*, **70**(6), 737-750. <https://doi.org/10.12989/sem.2019.70.6.737>
- Mohammadi, M., Saidi, A.R. and Jomehzadeh, E. (2010), "A novel analytical approach for the buckling analysis of moderately thick functionally graded rectangular plates with two simply-supported opposite edges", *Proc. Inst. Mech. Eng. Part CProc. Inst. Mech. Eng. Part C*, **224**, 1834-1841. <https://doi.org/10.1243/09544062JMES1804>
- Neves, A.M.A., Ferreira, A.J.M., Carrera, E., Cinefra, M., Roque, C.M.C., Jorge, R.M.N. and Soares, C.M.M. (2012a), "A quasi-3D hyperbolic shear deformation theory for the static and free vibration analysis of functionally graded plates", *Compos. Struct.*, **94**, 1814-1825. <https://doi.org/10.1016/j.compstruct.2011.12.005>
- Neves, A.M.A., Ferreira, A.J.M., Carrera, E., Roque, C.M.C., Cinefra, M., Jorge, R.M.N. and Soares, C.M.M. (2012b), "A quasi-3D sinusoidal shear deformation theory for the static and free vibration analysis of functionally graded plates", *Compos. Part B*, **42**, 711-725. <https://doi.org/10.1016/j.compositesb.2011.08.009>
- Nguyen, T.K. (2015), "A higher-order hyperbolic shear deformation plate model for analysis of functionally graded materials", *Int. J. Mech. Mater. Des.*, **11**(2), 203-219. <https://doi.org/10.1007/s10999-014-9260-3>
- Nguyen, D.K., Nguyen, Q.H., Tran, T.T. and Bui, V.T. (2017), "Vibration of bi-dimensional functionally graded Timoshenko beams excited by a moving load", *Acta Mech.*, **228**, 141-155. <https://doi.org/10.1007/s00707-016-1705-3>
- Pitakthapanaphong, S. and Busso, E.P. (2002), "Self-consistent elasto-plastic stress solutions for functionally graded material systems subjected to thermal transients", *J. Mech. Phys. Solids*, **50**, 695-715. [https://doi.org/10.1016/S0022-5096\(01\)00105-3](https://doi.org/10.1016/S0022-5096(01)00105-3)
- Pradhan, K.K. and Chakraverty, S. (2014), "Effects of different shear deformation theories on free vibration of functionally graded beams", *Int. J. Mech. Sci.*, **82**, 149-160. <https://doi.org/10.1016/j.ijmecsci.2014.03.014>
- Pradyumna, S. and Bandyopadhyay, J.N. (2008), "Free vibration analysis of functionally graded curved panels using a higher-order finite element formulation", *J. Sound Vib.*, **318**, 176-192. <https://doi.org/10.1016/j.jsv.2008.03.056>
- Reddy, J.N. (2011), "A general nonlinear third-order theory of functionally graded plates", *Int. J. Aerosp. Lightweight Struct.*, **1**, 1-21. <https://doi.org/10.3850/S201042861100002X>
- Safa, A., Hadji, L., Bourada, M. and Zouatnia, N. (2019), "Thermal vibration analysis of FGM beams using an efficient shear deformation beam theory", *Earthq. Struct.*, *Int. J.*, **17**(3), 329-336. <https://doi.org/10.12989/eas.2019.17.3.329>
- Sahouane, A., Hadji, L. and Bourada, M. (2019), "Numerical analysis for free vibration of functionally graded beams using an original HSDT", *Earthq. Struct.*, *Int. J.*, **17**(1), 31-37. <https://doi.org/10.12989/eas.2019.17.1.031>
- Salah, F., Boucham, B., Bourada, F., Benzair, A., Bousahla, A.A. and Tounsi, A. (2019), "Investigation of thermal buckling properties of ceramic-metal FGM sandwich plates using 2D integral plate model", *Steel Compos. Struct.*, *Int. J.*, **33**(6), 805-822. <https://doi.org/10.12989/scs.2019.33.6.805>
- Sekkal, M., Fahsi, B., Tounsi, A. and Mahmoud, S.R. (2017), "A new quasi-3D HSDT for buckling and vibration of FG plate", *Struct. Eng. Mech.*, *Int. J.*, **64**(6), 737-749. <https://doi.org/10.12989/sem.2017.64.6.737>
- Selmi, A. and Bisharat, A. (2018), "Free vibration of functionally graded SWNT reinforced aluminum alloy beam", *J. Vibroeng.*, **20**(5), 2151-2164. <https://doi.org/10.21595/jve.2018.19445>
- Shahrjerdi, A., Mustapha, F., Bayat, M. and Majid, D.L.A. (2011), "Free vibration analysis of solar functionally graded plates with temperature-dependent material properties using second order shear deformation theory", *J. Mech. Sci. Technol.*, **25**(9), 2195-2209. <https://doi.org/10.1007/s12206-011-0610-x>
- Simsek, M. (2010), "Vibration analysis of a functionally graded beam under a moving mass by using different beam theories", *Compos. Struct.*, **92**, 904-917. <https://doi.org/10.1016/j.compstruct.2009.09.030>
- Sina, S.A., Navazi, H.M. and Haddadpour, H. (2009), "An analytical method for free vibration analysis of functionally graded beams", *Mater. Des.*, **30**, 741-747. <https://doi.org/10.1016/j.matdes.2008.05.015>
- Sofiyev, A.H., Deniz, A., Akçay, I.H. and Yusufoglu, E. (2006), "The vibration and stability of a three-layered conical shell containing an FGM layer subjected to axial compressive load", *Acta Mechanica*, **183**, 129-144.

- <https://doi.org/10.1007/s00707-006-0328-5>
- Soliman, A.E., Eltaher, M.A., Attia, M.A. and Alshorbagy, A.E. (2018), "Nonlinear transient analysis of FG pipe subjected to internal pressure and unsteady temperature in a natural gas facility", *Struct. Eng. Mech., Int. J.*, **66**(1), 85-96.  
<https://doi.org/10.12989/sem.2018.66.1.085>
- Talha, M. and Singh, B.N. (2010), "Static response and free vibration analysis of FGM plates using higher order shear deformation theory", *Appl. Math. Model.*, **34**, 3391-4011.  
<https://doi.org/10.1016/j.apm.2010.03.034>
- Viswanathan, K.K., Javed, S. and Abdul Aziz, Z. (2013), "Free vibration of symmetric angle-ply layered conical shell frusta of variable thickness under shear deformation theory", *Struct. Eng. Mech., Int. J.*, **45**(2), 259-275.  
<https://doi.org/10.12989/sem.2013.45.2.259>
- Zhao, X., Lee, Y.Y. and Liew, K.M. (2009a), "Mechanical and thermal buckling analysis of functionally graded plates", *Compos. Struct.*, **60**, 161-171.  
<https://doi.org/10.1016/j.compstruct.2009.03.005>
- Zhao, X., Lee, Y.Y. and Liew, K.M. (2009b), "Free vibration analysis of functionally graded plates using the element-free kp-Ritz method", *J. Sound Vib.*, **319**, 918-939.  
<https://doi.org/10.1016/j.jsv.2008.06.025>